

Spectroscopic Survey of Field stars: A search for Metal-Poor stars

Sunetra Giridhar * and Aruna Goswami

Indian Institute of Astrophysics, Bangalore 560 034

2018 November 2

Abstract. We have undertaken a spectroscopic survey of field stars to find metal-poor objects among them. Though the main objective of the survey is to find new metal-poor stars, stellar parameterization is carried out for all the sample stars so that the other categories of interesting objects like composite stars, weak or strong CN, CH stars etc. can also be identified.

Observations are carried out using OMR spectrograph attached to VBT, Kavalur. The sample of candidate stars are chosen from prismatic survey of Beers and his collaborators covering a large part of the Galaxy. At the first phase of this project, the analysis is completed for a set of 19 relatively hot stars (T_{eff} in 6000 to 8000K range). The metallicities of the program stars are derived by synthesizing the spectrum in the wavelength range 4900 to 5400 Å for different metallicities and matching them with the observed spectra. This spectral region contains strong feature of FeI at 5269 Å and one moderately strong Fe I blend at 5228 Å. These features were generally relied upon for Fe/H determination. More than half of the candidate stars were found to show [Fe/H] in -0.7 to -1.2 range. Two most metal-poor stars have [Fe/H] values of -1.3 and -1.8. It appears that metal-poor candidates suggested by Beers et al. from their prismatic survey has a very significant fraction of metal-poor stars. The significantly metal-poor stars found so far would be studied in detail using high resolution spectra to understand nucleosynthesis processes that might have occurred in early Galaxy.

Keywords : Metal-poor stars, metallicity

*e-mail : giridhar@iiap.ernet.in

1. Introduction

Spectroscopic surveys containing large areas of the sky provide wealth of information on different groups of stars. Although finding new metal-poor stars is the prime objective of many surveys, many interesting objects like emission line objects, stars with unusually strong or weak CH, CN bands etc. are also discovered. Discovery and comprehensive studies of metal-poor stars in different Galactic locations are very important tools to study the structure and evolution of early Galaxy.

In the past, the surveys relied upon kinematic data for more efficient metal-poor star detection and hence the objects were chosen from the proper-motion catalogues. It was pointed out by Carney (1997) and others that for complete understanding of disk-halo structure, the kinematic bias should be avoided.

Objective prism survey of Beers, Preston and Shectman (1992) called HK survey covers large portion of the sky in northern and southern hemispheres. Hamburg/ESO survey covers a much larger portion of the sky though it is restricted to the southern hemisphere. Edinburgh -Cape blue object survey of Stobie et al. 1997 (hereinafter EC) covers most of the high galactic latitude southern sky objects.

In our earlier work (Giridhar, et al. 2001), we have carried out spectroscopic investigation of stars selected from the HK survey and from a list of stars with tangential velocity in excess of 100 kms^{-1} published by Lee (1984). We found the stars from HK survey to be considerably metal-poor, but the stars taken from Lee's table were not very promising metal-poor candidates.

2. Selection of Program stars

The program stars listed in Table 1, are mostly taken from the EC survey.

EC survey was initiated to study distant hot stars from their photographic photometry. While picking hot stars in B versus (U-B) diagram, some F and G stars which are in fact metal-poor were mistaken as blue objects. The U colours had become brighter due to decreased absorption from otherwise strong metal lines. A shorter list (of nearly 600 stars) of such contaminating (but interesting) objects was supplied by Beers et al. (2001) from which stars in the magnitude range 11-14 mag were observed at VBT using OMR spectrograph. In addition to these objects, spectrophotometric and radial velocity standards were also observed. In this paper, we present the results obtained at the first phase of an ongoing spectroscopic survey program.

Broadband UBV colours of the EC stars are available in Beers et al. (2001). The errors in this photoelectric photometry are in the range of 0.02 to 0.04. These authors

Table 1: EC stars and standards observed with VBT

Star	V	<i>l</i>	<i>b</i>	RA (2000)	DEC (2000)
EC 05148-2731	12.69	229.9	-31.8	05:16:50.7	-27:28:25
EC 10488-1244	11.15	263.1	40.4	10:51:18.6	-13:00:28
EC 10004-1405	13.65	253.1	31.8	10:02:54.5	-14:19:41
EC 10292-0956	12.06	255.9	39.6	10:31:44.9	-10:11:36
EC 11091-3239	12.56	279.8	25.4	11:11:32.6	-32:56:17
EC 11175-3214	12.55	281.5	26.5	11:19:58.8	-32:30:34
EC 11553-2731	11.29	288.7	33.6	11:57:55.3	-27:48:22
EC 11260-2413	12.85	279.9	34.6	11:28:29.8	-24:29:38
EC 12245-2211	13.96	295.6	40.1	12:27:07.8	-22:27:44
EC 12418-3240	12.19	301.3	29.9	12:44:32.6	-32:57:15
HD 86801	8.79	200.5	52.6	10:01:34.9	+28:34:00
HR 5694	5.10	3.7	46.4	15:19:18.7	+01:45:55.4
EC 12473-1945	10.43	302.5	42.8	12:49:57.0	-20:02:04
EC 12473-1711	11.68	302.4	45.4	12:49:58.3	17:27:44
EC 12477-1724	11.40	302.6	45.2	12:50:24.1	-17:40:20
EC 12493-2149	13.51	303.1	40.8	12:51:58.6	-22:06:09
EC 13042-2740	12.95	307.1	34.8	13:06:55.8	-27:56:29
EC 13501-1758	12.63	322.8	42.3	13:52:50.7	-18:13:21
HR 5384	6.30	347.2	56.0	14:23:15.2	+01:14:29.6
EC 13506-1845	12.87	322.6	41.5	13:53:21.7	-19:00:32
EC 13564-2249	12.78	322.6	37.2	13:59:15.3	-23:03:36
EC 13567-2235	12.60	322.8	37.4	13:59:29.8	-22:49:57
EC 13586-2220	13.72	323.4	37.5	14:01:27.4	-22:34:41
EC 14005-2224	13.33	323.9	37.3	14:03:22.8	-22:38:50
EC 15473-1241	13.11	356.1	31.1	15:50:06.8	-12:50:11
HR 4054	4.80	217.1	54.4	10:19:44.1	+19:28:15

have estimated reddening by interpolation in the tables of Burstein & Heiles (1982). The reddening estimates have uncertainties of $\sim \pm 0.03$.

3. Observation and Data analysis

The spectrograph used for observation is the OMR Spectrograph designed and built by the Optomechanics Research Inc., Vail, Arizona, USA. It is available at the Cassegrain focus of the 2.3m Vainu Bappu Telescope (VBT) at Kavalur (Prabhu, Anupama & Surendiranath 1998). With a 600 lmm^{-1} grating, we get a dispersion of 2.6 \AA per pixel. The detector is Tetrionix 1K CCD with $24 \mu\text{m}$ pixels. Wavelength calibration was done with the help of Fe-Ar hollow cathode lamp. Flat field correction was done using Tungsten-Halogen Quartz lamp. The spectroscopic reduction steps were carried out using

various tasks included in the NOAO package of IRAF. At a resolution of 1000, one can only measure the strengths of blends around strong features like hydrogen lines, Ca II H, K lines etc. Although we could identify a few high radial velocity objects, good radial velocity measurements using the cross-correlation technique could not be made as the radial velocity standards observed with the same setup were not of the same spectral types as program stars for some nights. We, therefore, do not report the radial velocities though good measurements exist for one third of the sample.

4. Determination of the stellar parameters

Firstly, we have attempted a preliminary classification of these unknown objects. Towards this objective, we were guided by a library of stellar spectra published by Jacoby, Hunter and Christian 1984. This library contains 161 flux calibrated spectra of O-M stars covering luminosity class I to V. Most of these stars are of luminosity types I, III and V with a very few stars of type II.

We have chosen this collection of standard stars primarily because, these spectra are observed with nearly the same resolution as the spectra obtained by us at VBT. Catalogue stars used for our purpose are listed in Table 2.

We have normalised spectra of the catalogue as well as our program stars by dividing it by the continuum. On these normalised spectra we measured the strength of several features (Table 2) that are known to be good indicators of spectral type (and hence temperature), and luminosity class.

Hydrogen line strengths, particularly the higher members of Balmer series show different locii for different luminosity classes in line strength versus (B-V) plot. Figure 1 shows the variations of these features as a function of $(B-V)_o$. We did not use Ca II K feature as this feature gets contaminated by H_ϵ for A type stars. Figure 1 also shows the polynomial fit for the strengths of hydrogen lines. The same curves (polynomial fit to the catalogue stars of Jacoby et al. 1984) are retained in Figure 2 but the data points are of the EC stars observed by us.

Strengths of the observed features for the program stars and the standard stars observed with OMR spectrograph are presented in Table 3. The features Ca II H and K lines, Ca I line at 4226\AA and MgI+FeI blend at 5170\AA are strongly dependent on temperature and hence show steep variations when plotted as a function of $(B-V)_o$. Ca features show a linear relation with (B-V) with no significant distinction between luminosity types. The Mg I features in $5167\text{-}5184\text{\AA}$ region show strong luminosity dependence at temperatures cooler than 6500K.

Using the hydrogen lines strengths, the first estimates of the spectral types and lu-

Table 2: Line strengths in Å measured for the Catalogue stars

Star	$(B - V)_o$	Sp type	Ca II K	Ca II H	H_δ	Ca I	H_γ	H_β	Mg+Fe	Mg+Fe	Fe I
			3934	3969	4102	4227	4340	4861	5171	5184	5270
HD 9547	0.30	A5V	—	—	12.8	0.7	12.4	13.8	1.3	0.4	1.5
HD 10032	0.33	F0V	6.0	9.2	7.3	0.9	6.2	8.0	1.5	0.7	1.7
HD 23733	0.34	A9V	6.6	10.1	8.3	0.8	7.2	8.4	1.3	0.6	2.3
SAO 57199	0.40	F6V	9.9	10.3	4.1	1.1	4.6	4.6	2.0	1.0	1.1
HZ 948	0.47	F3V	7.4	7.8	5.3	0.8	5.3	4.9	1.8	0.6	2.0
HD 5702	0.49	F7V	10.8	10.2	4.0	1.5	3.9	4.8	2.1	1.1	2.0
HD 107132	0.50	F7V	11.3	10.8	4.3	1.2	3.3	3.8	2.0	1.0	2.7
HZ 227	0.52	F5V	8.9	8.93	5.7	0.7	5.0	6.8	1.9	1.1	1.2
HR 5694	0.54	F8IV	10.2	9.3	4.9	0.9	3.4	4.8	1.9	0.8	—
HD 6111	0.55	F8V	12.1	10.9	3.3	1.4	3.5	3.4	2.4	1.4	—
HD 107399	0.56	F9V	13.3	12.2	2.7	1.6	2.9	3.7	2.4	1.3	2.7
HD 31084	0.57	F9V	13.0	9.2	3.7	1.3	3.1	3.8	2.5	1.2	—
HD 107214	0.58	F7V	11.0	9.2	3.5	1.5	3.9	4.0	2.3	1.3	—
HD 66171	0.60	G2V	13.1	11.0	2.3	1.9	2.6	2.6	3.1	1.6	—
HD 17647	0.61	G1V	13.9	10.5	2.5	2.3	3.0	2.8	3.4	2.0	3.7
HR 5384	0.63	G1IV	12.9	10.0	3.3	1.4	3.0	3.5	3.0	1.7	—
BD 58199	0.64	G3V	14.8	11.6	2.1	1.9	3.8	2.5	3.1	2.0	2.5
HD 28099	0.66	G0V	8.7	12.2	5.8	1.3	4.0	3.6	3.3	1.7	4.0
HD 22193	0.71	G6V	13.6	10.0	2.3	2.3	3.0	2.6	3.8	2.0	3.7
TrA 14	0.74	G4V	14.0	12.0	2.1	1.2	2.0	1.7	1.8	1.5	2.6
HD 12027	0.22	A3III	3.3	—	13.8	0.4	16.3	18.4	1.3	0.3	—
HD 12161	0.23	A8III	4.8	11.3	12.5	0.6	8.1	11.9	1.6	0.5	0.8
HD 240296	0.25	A6III	5.6	8.2	9.3	1.2	9.0	9.0	1.7	0.4	1.7
HD 64191	0.28	F0III	6.6	10.5	10.8	0.6	9.9	7.1	1.4	0.7	1.3
BD 003227	0.40	F5II	8.7	9.2	4.8	0.8	4.2	4.6	1.8	1.0	2.0
HD 56030	0.45	F6III	8.9	9.2	3.9	1.3	3.6	4.5	2.4	0.8	1.5
BD 610367	0.46	F5III	8.7	9.4	5.9	1.5	5.2	5.8	1.4	0.7	2.8
HD 5211	0.47	F4III	10.0	9.9	5.1	1.1	4.5	5.0	1.8	0.8	1.3
SAO 20603	0.48	F7III	11.4	9.9	3.7	1.2	3.9	4.4	2.3	1.0	2.8
HD 9979	0.50	F8III	14.1	12.2	3.4	2.3	3.0	3.1	3.5	2.0	1.9
BD 302347	0.58	G0III	13.6	10.5	3.5	1.6	3.3	3.8	2.6	1.2	2.8
HD 15866	0.66	G0III	12.5	11.8	3.0	1.5	2.8	4.0	2.6	1.4	3.4
HD 25894	0.71	G2III	13.1	10.4	3.0	2.1	2.6	2.9	3.8	2.0	4.1
HD 2506	0.89	G4III	18.6	13.0	1.9	2.3	1.9	2.0	2.8	1.2	3.0
HR 4786	0.89	G5III	17.2	12.3	2.2	1.2	2.0	3.1	3.1	1.1	—
BD 281885	0.91	G5III	17.7	15.0	1.7	3.0	2.6	2.5	3.5	1.8	4.2
HD 249384	1.03	G8II	18.0	16.6	1.8	2.9	2.4	1.4	4.6	2.9	4.0
HD 250368	1.04	G8II	14.0	12.0	1.6	1.9	1.8	1.4	3.9	2.0	4.0
SAO 12149	0.07	A1I	1.4	5.4	4.7	0.4	4.4	4.8	0.9	0.1	0.7
SAO 12096	0.13	A4I	5.4	9.5	7.3	0.7	7.3	8.2	1.2	0.4	—
HD 842	0.14	A9I	6.6	10.1	8.9	0.8	7.9	10.0	1.5	0.6	2.2
SAO 37370	0.16	F0Ib	6.7	9.9	7.1	0.6	6.3	7.5	1.3	0.6	2.3
42LSI	0.17	A2I	6.5	7.7	9.1	0.7	7.2	7.8	1.5	0.5	2.2
HD 9167	0.18	A7I	6.5	8.6	6.1	0.7	5.9	5.6	1.4	0.4	2.6
BD 580204	0.21	F2I	8.5	10.9	7.1	0.7	7.6	7.8	1.3	0.6	2.8
SAO 21536	0.28	F4I	9.1	11.8	5.7	0.9	6.3	6.9	2.0	—	3.1
HD 9973	0.30	F5Iab	13.0	12.7	5.4	1.9	5.7	5.2	2.7	1.2	4.4
HD 8992	0.31	F6Ib	13.0	14.9	4.0	2.0	4.9	4.3	2.2	0.8	—
HD 187428	0.56	F8Ib	14.0	13.47	3.2	1.3	4.3	4.1	2.4	0.9	3.8
HD 17971N	0.60	F7I	12.9	12.0	4.3	1.4	4.9	6.1	2.9	1.2	3.2
HD 25361	0.88	G0Ia	15.5	13.2	2.4	1.8	3.5	3.8	2.5	1.6	4.7
SAO 21446	0.91	G1I	18.4	14.0	2.1	2.2	3.3	3.2	2.2	1.0	5.2

Calibrating Stars

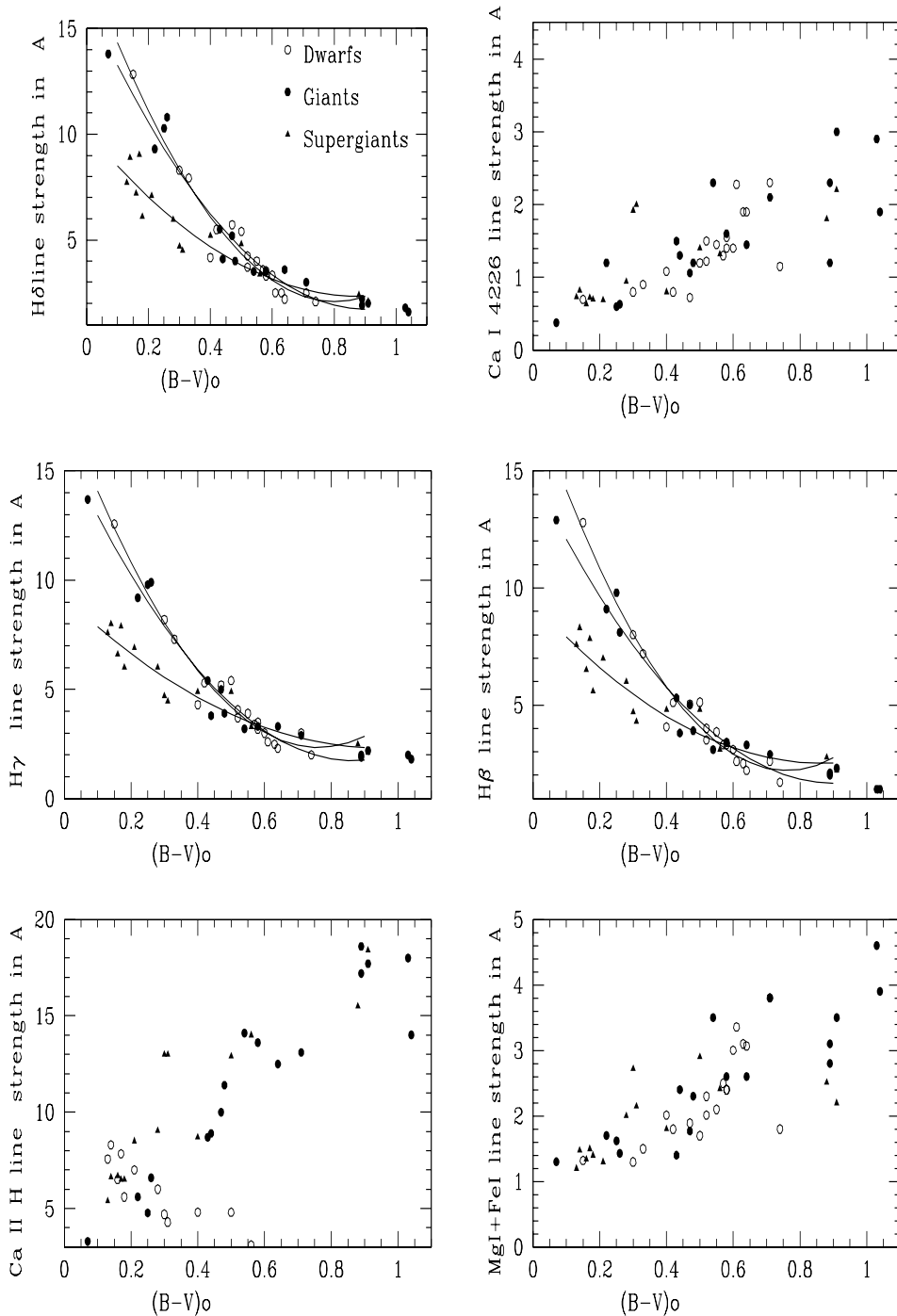


Fig.1 : Strengths of different spectral features as a function of $(B-V)_0$ for the stars from the Catalogue of Jacoby et al. The symbols for all the six panels have the same meaning as given in the panel 1.

EC Stars and standards

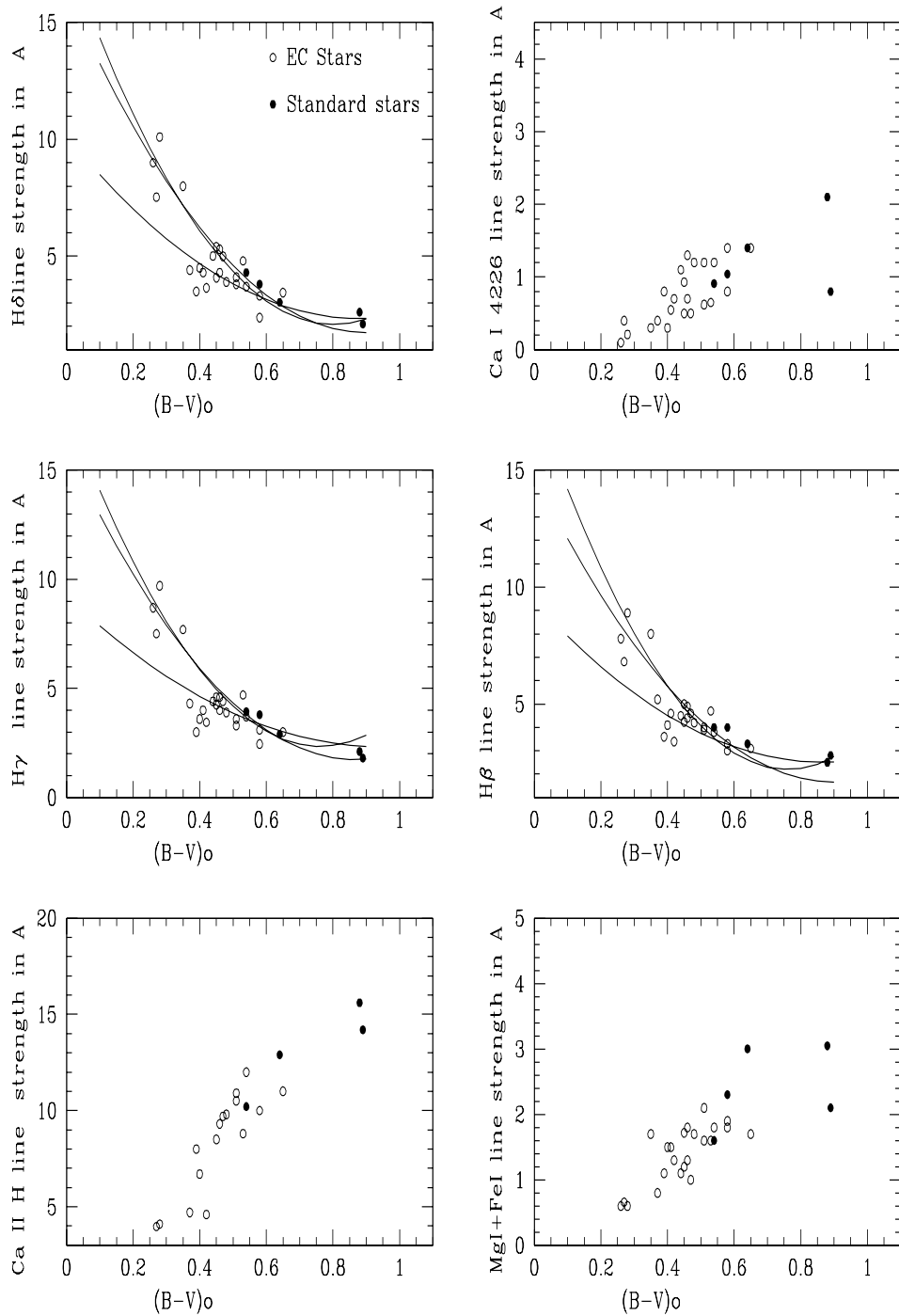


Fig. 2 : Strengths of different spectral features as a function of $(B-V)_o$ for the stars observed by us with VBT. The symbols for all the six panels have the same meaning as given in the panel 1.

Table 3: Strengths of observed features in Å for the program stars and standards

Star	$(B - V)_o$	Ca II K	Ca II H	H_δ	Ca I	H_γ	H_β	Mg+Fe	Mg+Fe	Fe I
		3934	3969	4102	4227	4340	4861	5171	5184	5270
EC 05148-2731	0.28	4.1	—	10.1	0.2	9.7	8.9	0.6	0.2	0.5
EC 10488-1244	0.45	8.5	8.4	5.4	0.5	4.6	5.0	1.2	0.8	1.5
EC 10004-1405	0.40	6.7	—	4.5	0.3	3.6	4.1	1.5	0.6	1.4
EC 10292-0956	0.54	12.0	10.0	3.7	1.2	3.7	3.8	1.8	1.1	1.7
EC 11091-3239	0.47	9.7	8.4	5.0	0.5	4.4	4.6	1.0	0.4	1.5
EC 11175-3214	0.35	—	—	8.0	0.3	7.7	8.0	1.7	0.7	1.9
EC 11553-2731	0.41	—	—	4.3	0.6	4.0	4.6	1.5	0.7	1.4
EC 11260-2413	0.26	1.7	—	9.0	0.1	8.7	7.8	0.6	0.1	0.3
EC 12245-2211	0.44	—	—	5.0	1.1	4.4	4.5	1.1	—	1.3
EC 12418-3240	0.58	10.0	9.0	3.3	1.4	3.1	3.3	1.8	0.7	2.1
HD 86801	0.58	—	—	3.8	1.0	3.8	4.0	2.3	1.3	2.2
HR 5694	0.54	10.2	9.3	4.3	0.9	3.9	4.0	1.6	1.0	1.7
EC 12473-1945	0.51	10.5	9.3	3.8	0.6	3.6	4.0	1.6	0.6	1.8
EC 12477-1711	0.53	8.8	8.3	4.8	0.7	4.7	4.7	1.6	0.8	1.7
EC 12477-1724	0.46	—	—	5.3	0.7	4.6	4.9	1.8	1.4	2.1
EC 12493-2149	0.58	—	—	2.4	0.8	2.5	3.0	1.9	1.0	2.4
EC 13042-2740	0.45	—	—	4.1	0.9	4.3	4.2	1.7	1.4	1.8
EC 13501-1758	0.65	11.0	9.3	3.5	1.4	3.0	3.1	1.7	1.0	2.4
HR 5384	0.64	12.9	10.0	3.0	1.4	2.9	3.3	3.0	1.8	2.6
EC 13506-1845	0.48	9.8	—	3.9	1.2	3.9	4.2	1.7	1.0	2.1
EC 13564-2249	0.51	10.9	9.8	4.1	1.2	3.3	3.9	2.1	1.2	1.5
EC 13567-2235	0.46	9.3	8.4	4.3	1.3	4.0	4.4	1.3	0.6	1.0
EC 13586-2220	0.37	4.7	6.4	4.4	0.4	4.3	5.2	0.8	0.6	1.1
EC 14005-2224	0.42	4.6	7.0	3.7	0.7	3.5	3.4	1.3	0.4	0.7
EC 15473-1241	0.27	4.0	8.0	7.5	0.4	7.5	6.8	0.7	0.1	0.4
HR 4786	0.89	14.2	12.3	2.1	0.8	1.8	2.8	2.1	1.0	3.0

minosity classes were made for the program stars. The standard stars observed were also analysed in an identical way. The comparison of the results obtained by us with the published ones for the standard stars lead us to believe that the spectral types are accurate to ± 2 subtypes. Since the bulk of classifying stars belong to luminosity classes V, III and I with a very few of type II, the errors are difficult to estimate for luminosity types. We have used luminosity types determined above, the $(B-V)_o$ from Beers et al.(2001) and the calibration of Schmidt- Kaler (1982) to derive T_{eff} of the program stars. Our estimates of T_{eff} and $\log g$ (estimated from the luminosity types) that are based on the hydrogen line strengths are presented in columns 4 and 6 respectively of Table 4 under the subheading H.

Table 4: Derived Atmospheric Parameters and Metallicities

Star	Sp Type	LC	T_{eff}	T_{eff}	$\log g$	$\log g$	$(B - V)_o$	M_v	Dist.	$[Fe/H]$	Z
			H	S	H	S				S	kpc
EC 05148-2731	F0	IV	7500	8250	3.6	4.0	0.28	1.7	1.58	-0.6	0.76
EC 10488-1244	F5	III	6500	6500	3.0	2.75	0.45	1.6	0.79	-1.0	0.47
EC 10004-1405	F3	IV	6500	7300	2.5	4.0	0.40	2.5	1.69	-0.7	0.81
EC 10292-0956	F9	IV	6100	6000	3.5	4.25	0.54	2.8	0.71	-1.2	0.41
EC 11091-3239	F6	IV	6400	6500	3.0	4.25	0.47	2.7	0.93	0.0	0.36
EC 11175-3214	F2	IV	6900	7300	4.0	3.5	0.35	2.0	1.26	-0.5	0.51
EC 11553-2731	F3	IV	6500	6800	3.0	4.0	0.41	2.5	0.57	-0.5	0.29
EC 12245-2211	F5	III	6500	6800	3.0	3.0	0.44	1.6	2.96	-1.0	1.74
EC 12418-3240	G0	IV	6100	6000	4.0	4.0	0.58	3.0	0.79	-0.9	0.35
EC 12473-1945	F8	III	6200	6300	3.5	3.75	0.51	1.6	0.58	-0.9	0.36
EC 12477-1711	F8	III	6200	6300	3.5	3.75	0.53	1.8	0.95	-0.8	0.62
EC 12477-1724	F6	IV	6400	6500	4.0	4.25	0.46	2.6	0.57	-0.5	0.36
EC 12493-2149	G0	V	6000	6000	4.5	5.0	0.58	4.3	0.69	-0.7	0.41
EC 13042-2740	F6	III	6300	6300	2.0	3.0	0.45	1.5	1.95	-1.0	1.01
EC 13501-1758	G0	IV	5800	5500	3.0	4.0	0.65	3.0	0.84	-1.3	0.52
EC 13506-1845	F6	III	6300	6300	3.0	3.0	0.48	1.6	1.79	-0.7	1.08
EC 13564-2249	F7	III	6200	6000	2.0	3.5	0.51	2.0	1.43	-0.9	0.78
EC 13567-2235	F6	III	6300	6500	2.0	3.0	0.46	1.6	1.58	-1.0	0.87
EC 13586-2220	F3	III	6700	6800	2.5	3.0	0.37	1.6	2.62	-1.8	1.45
Standard Stars											
HR 4054	F6	IV	6300	6300	3.9	4.0	0.45	2.6	0.026	0.0	0.01
HD 86801	G0	V	6050	5800	4.5	4.75	0.58	4.3	0.079	-1.2	0.06
HR 5694	F8	IV	6200	6300	4.0	4.0	0.54	2.9	0.027	-0.2	0.02
HR 5384	G1	V	5800	5800	4.5	4.25	0.64	4.9	0.019	-0.4	0.01

5. Spectrum Synthesis

Starting with these values of T_{eff} and $\log g$ derived in the last section we decided to further refine these parameters and also to derive metallicity by using line and spectrum synthesis method.

5.1 Sensitivity of Mg I features at 5167-5184 Å

The three Mg I features in 5167-5184Å region were found to be very sensitive to temperature and gravity changes but show stronger dependence on gravity for stars cooler than 6500K. We have computed the line strengths of these features using 2000 version of

spectrum synthesis program written by Sneden (first version described in Sneden 1973) and using models of Kurucz (1993) covering a large range in T_{eff} and $\log g$. We show in the figure 3 computed blend equivalent widths (sum of equivalent widths for the three Mg I lines) of Mg I features in 5167-5184 Å for models of different temperatures and gravities. This figure was found very useful in the refinement of temperature and gravity estimates particularly the gravity.

5.2 Final atmospheric parameters and estimation of [Fe/H]

We have synthesized the spectral regions around 4900-5400Å and redetermined more accurately, the stellar parameters T_{eff} and $\log g$ as well as metallicity [Fe/H] for the program stars. We were guided by Figure 3 in improving the gravity estimates. For synthesizing the spectral regions we have generated a linelist using NIST data base, supplemented by linelists of Thevenin (1989, 1990), unpublished compilation of R.E. Luck and linelist database of Kurucz. For checking the accuracy of atomic data, mainly the oscillator strengths used in the linelist, we had synthesized the solar spectrum around the spectral region of our interest using the solar model of Holweger and Muller (1974). A fairly good reproduction of the solar spectrum obtained using this linelist lent support to our belief that the linelist was satisfactory. We have further tested the linelist by computing the above mentioned spectral regions for two standard stars, HR 5384 and HR 5694, of known stellar parameters. A temperature of $T_{eff} \sim 5640\text{K}$ and metallicity [Fe/H] = -0.20 was estimated for HR 5384 by Lebreton et al. (1999). Cayrel de Stobel et al. (1992) had reported temperature range $T_{eff} \sim 5950$ to 6260 K, $\log g \sim 3.9$ to 4.0 and metallicity [Fe/H] ~ -0.6 to 0.06 for HR 5694. A synthetic spectrum obtained using the adopted linelist and a stellar model with T_{eff} of 5800K , $\log g = 4.25$ and metallicity [Fe/H] = -0.22 could reproduce the observed spectrum of HR 5384 fairly in good agreement. Similarly, a synthetic spectrum obtained using a stellar model with T_{eff} of 6300 and $\log g = 4.0$ could also reproduce the observed spectrum of HR 5694. These agreements are illustrated in figure 4 along with the synthetic spectra of two other standard stars, HR4054 and HD86801, all well-known radial velocity standards.

For spectral synthesis of the program stars we have started with atmospheric models of Gustafsson et al. (1975), and Kurucz (1993) at T_{eff} and $\log g$ estimated from the hydrogen line strengths. The gravity estimates were further refined with the help of figure 3.

Starting from solar metallicity models, the value of [Fe/H] is gradually changed to obtain a best fit of the observed spectrum. While changing [Fe/H], [X/H] of the elements which are identified as having maximum contributions in the spectral region of our interest , such as Mg, Ca, Ti, Ni are also correspondingly changed. For this, we have made use of [Fe/H] vs [X/H] compiled from various sources and compared with their evolutionary calculations by Goswami and Prantzos (2000, fig 7). The observed data has large scatter in [Fe/H] range -0.5 to 0.0. For our purpose of spectral synthesis we have adopted an

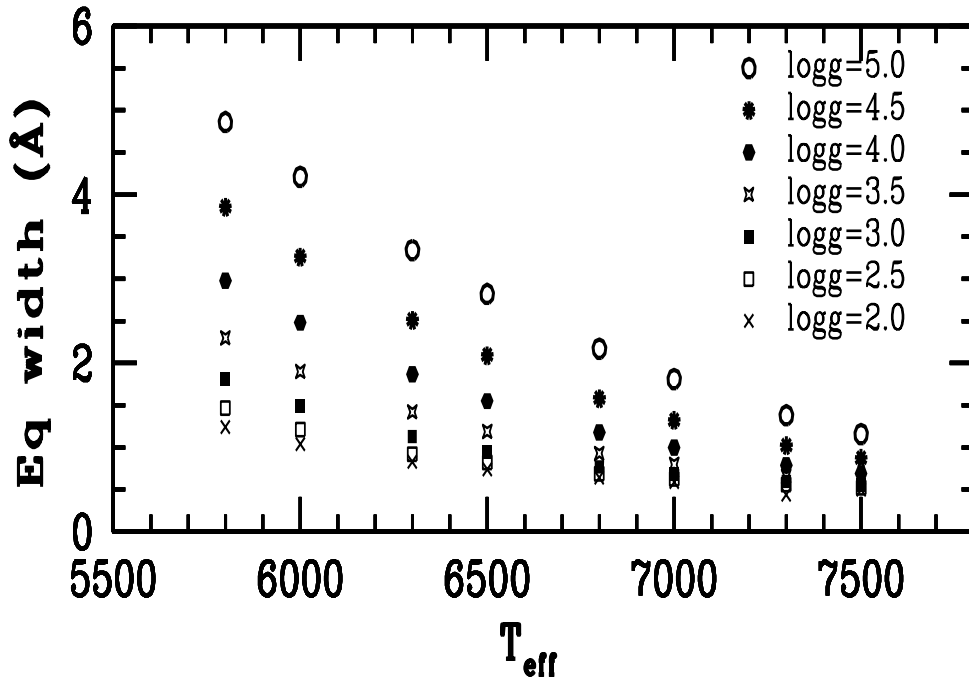


Fig. 3 : Computed equivalent widths (in Å) for Mg I feature at 5174-5183 Å for different temperatures and gravities. Each point corresponds to combined equivalent width of three Mg I lines that form this feature.

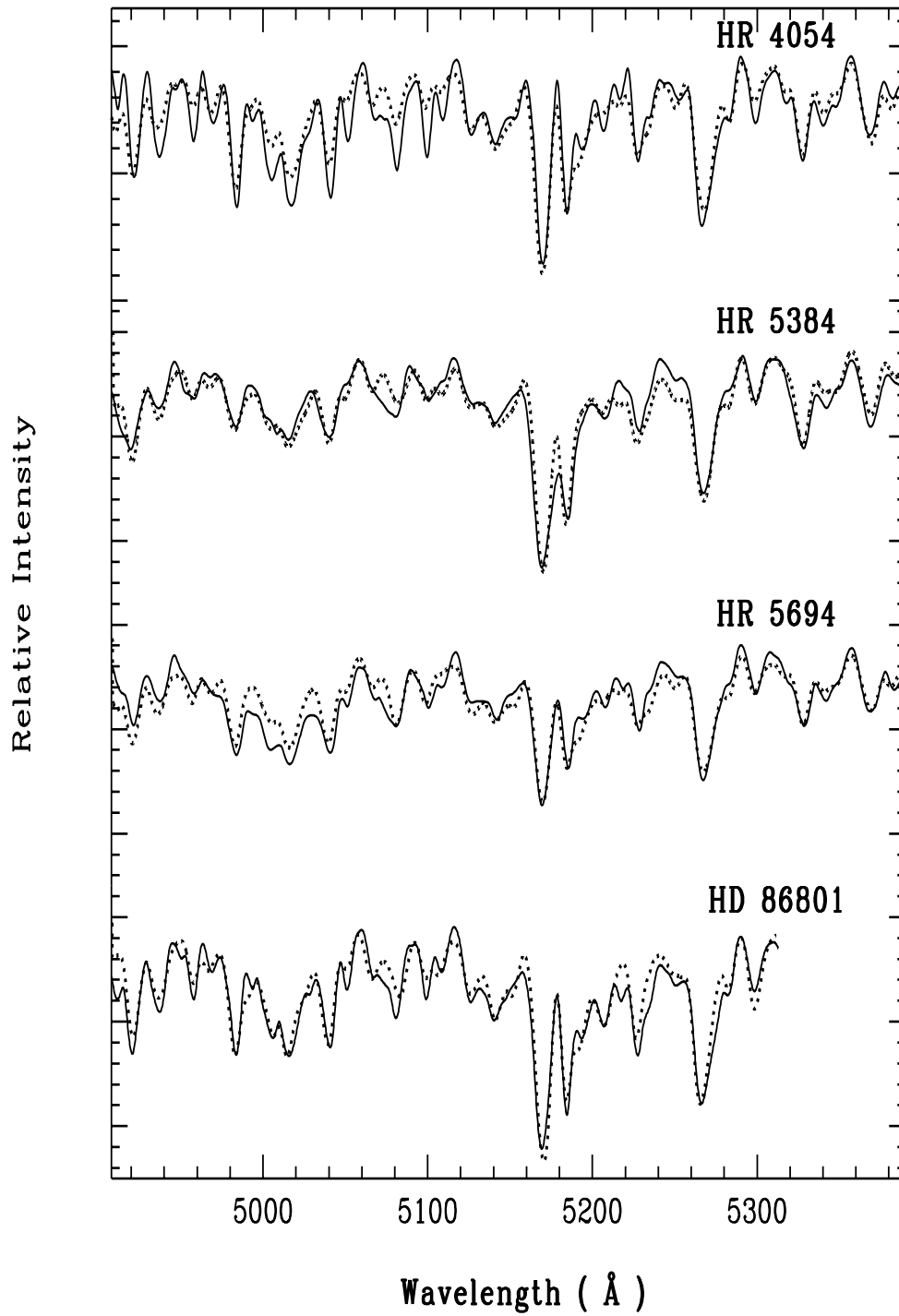


Fig. 4: The observed spectra (shown by continuous line) of standard stars compared with synthesized spectra.

average value of $[X/Fe]$ corresponding to $[Fe/H]$. In figures 5 and 6 we present synthetic spectra for several of our program stars compared with their observed spectra. The results are presented in Table 4, where H and S denote atmospheric parameters derived from hydrogen lines strengths and spectral synthesis respectively.

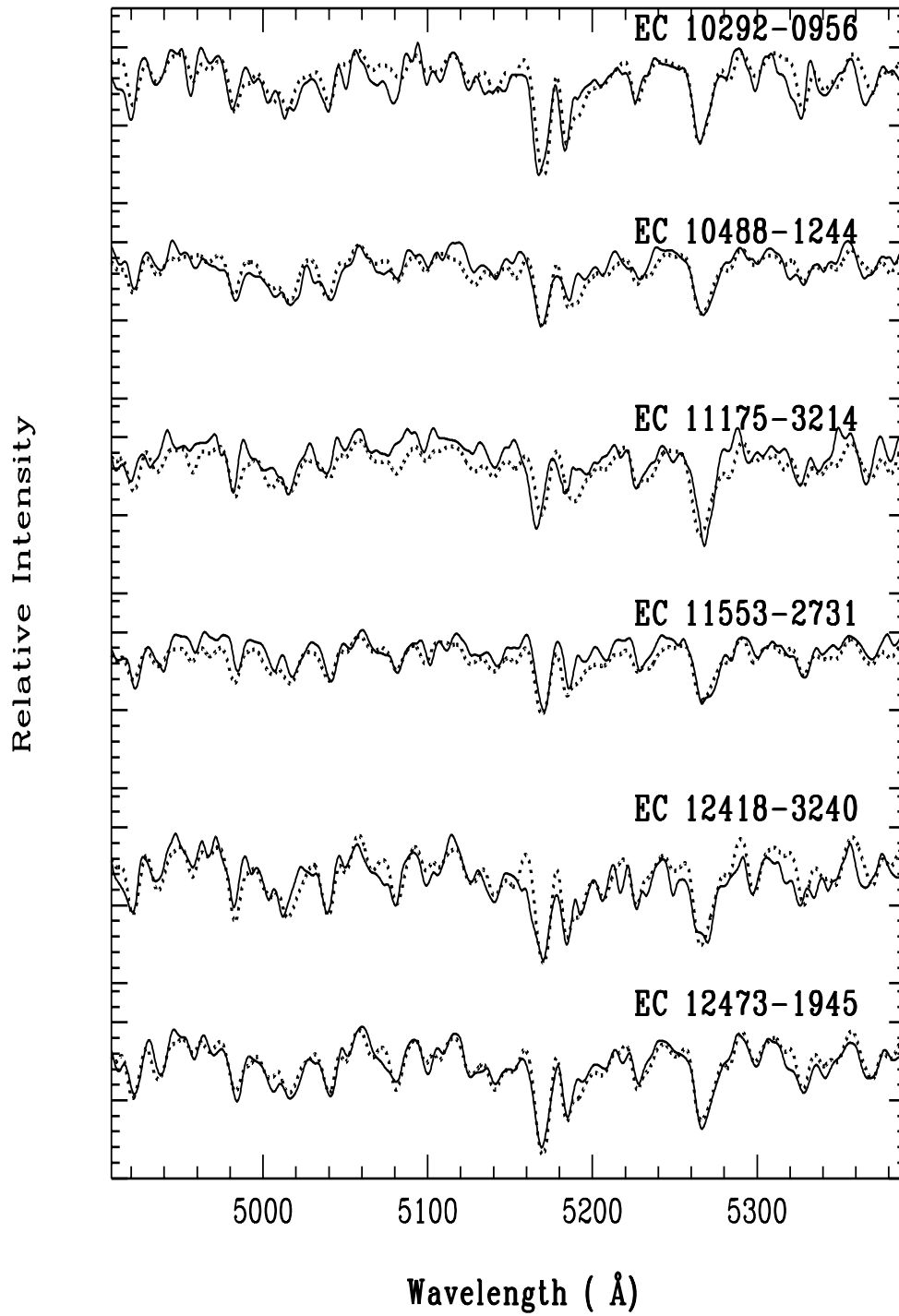
The agreement between the derived T_{eff} and $\log g$ from the two approaches is not very satisfactory for the stars hotter than 7000K but is very good for stars in 6000- 7000K temperature range where most of the sample stars belong to. For majority of stars T_{eff} agrees within $\pm 200K$. We seem to derive systematically higher value of gravity from spectrum synthesis but we are more inclined to believe higher values as Mg I feature is known to be a good gravity indicator as illustrated in Figure 3. Secondly, the calibrating stars in Jacoby's catalogue did not have uniform distribution in the luminosity classes. We believe our $[Fe/H]$ estimates for stars in T_{eff} 5800-7000K are accurate within ± 0.3 dex.

Perhaps for hotter stars one requires non-LTE models and a linelist tested for completeness using some well studied hot star like Vega. It is likely that for EC 05148-2731 and EC 10004-1405 the estimated $[Fe/H]$ may have uncertainty larger than ± 0.3 .

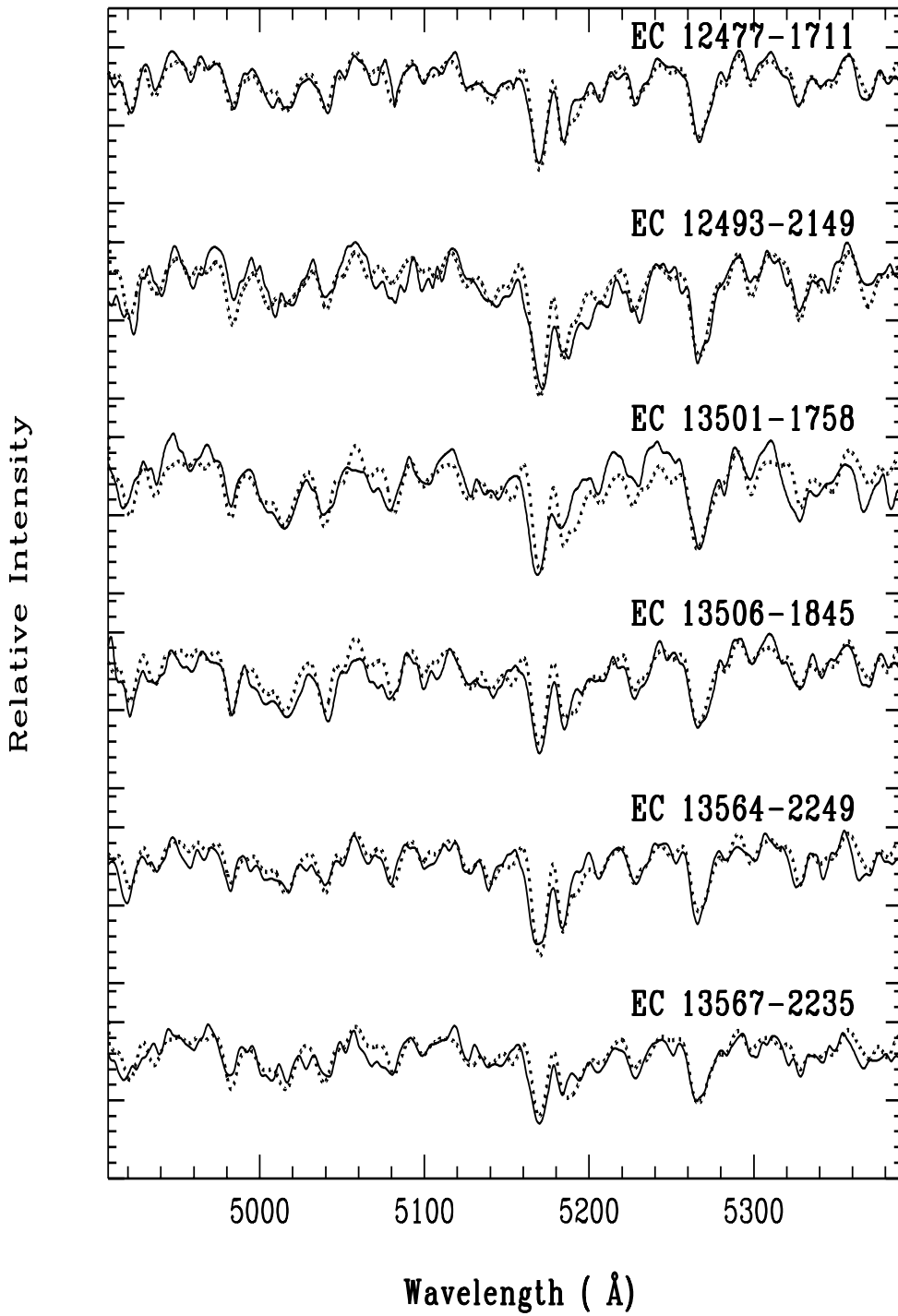
From the spectroscopic estimates of T_{eff} and $\log g$ and calibration of Schmidt-Kaler we have estimated absolute magnitude and hence the distances that are also presented in Table 4. The last column of the Table 4 shows the distance above the galactic plane in kpc. The last four entries in the table are the radial velocity standards observed with the same setup. For HR 5384 and HR 5694 the atmospheric parameters and $[Fe/H]$ are in close agreement with the published values. No previous $[Fe/H]$ estimate exists for HD 86801. For EC 10488-1244, EC 10004-1405 and EC 10292-0956, Prof. T.C. Beers had sent us unpublished $[Fe/H]$ estimates of -1.1, -0.8 and -1.4 that are in very good agreement with values -1.0, -0.7 and -1.2 derived by us though his estimate is based upon the strength of Ca II K line.

6. Results and Conclusions

It is obvious from the Table 4 that the bulk of the stars chosen from the EC survey belong to spectral type range A9 to F7. A large fraction of them are dwarfs or subgiants and the rest are giants. Sample stars EC12477-1724, EC10004-1405, EC11260-2413 have radial velocities in excess of 100 km s^{-1} ($+230, +138, -100 \text{ km s}^{-1}$) $\pm 15 \text{ km s}^{-1}$ respectively. However, they are not the most metal-poor objects. In fact the significantly metal-poor stars like EC 13586-2220, EC 13501-1758 and EC 10292-0956 are not the high velocity objects (radial velocity is less than 50 km s^{-1}). Hence the high velocity is not a very robust criteria for searching new metal-poor stars. From the inspection of galactic coordinates and derived distances, it appears that the sample stars are distributed in the thick disk around the local spiral arm. The most metal-deficient star EC 13586-2220 with



Figs. 5: The observed spectra (shown by continuous line) of program stars compared with synthesized spectra.



Figs. 6: The observed spectra (shown by continuous line) of program stars compared with synthesized spectra.

Galactic longitude 323° and distance of 2.6 kpc, possibly lies in the direction of interarm region between the local and Sagittarius arm. With a distance of 1.45 kpc above the Galactic plane, it might be beyond the thick disk. Nearly half the sample stars covered in the present work turned out to be significantly metal-poor with $[\text{Fe}/\text{H}]$ in -0.7 to -1.2 range. EC 13586-2220, EC 13501-1758 and EC 10292-0956 are the most metal-poor objects in the sample with $[\text{Fe}/\text{H}]$ of -1.8, -1.3 and -1.2 respectively. We intend to carry out a complete analysis of these three objects using high resolution spectra. Though the present sample is not very extensive, we do not see strong dependence of metallicity on the Z. We conclude that the objects presented in EC survey are promising candidates for metal-poor stars and detailed investigation of a larger sample will lead to a better understanding of the galactic structure and that of early Galactic history. The present work presents the initial phase of an ongoing survey program.

Acknowledgements

We are grateful to Prof. T.E. Beers for sending us the list of candidate stars and his unpublished $[\text{Fe}/\text{H}]$. We also thank Prof. D. L. Lambert for useful comments on the manuscript. We are grateful to VBT staff members for their kind help in getting observations and also to an anonymous referee whose comments have led to a much better presentation of the material in this paper.

References

- Beers, T. C. , Preston, G. W. , Shectman, S. A., 1992, *AJ*, **103**, 1987.
 Beers T.C., Rossi, S., Donoghue, D. O., Killkenny, D., Stobie, R. S., Koen, C., Wilhelm, R., 2001, *MNRAS*, **320**, 451.
 Burstein, D., Heiles, C., 1982, *AJ*, **87**, 1165.
 Carney, B. W., 1997, In "Proper Motions & Galactic Astronomy", *ASP Conf. Ser.* Vol **127**, 117.
 Cayrel De Strobel G., Hauck, B., Francois, P., Thevenin, F., Friel, E., Mermilliod, M., Borde, S., 1992, *A&AS*, **95**, 273.
 Giridhar, S., Lambert, D. L., Gonzalez, G., Pandey G. 2001, *PASP*, **113**, 519 .
 Goswami, A. & Prantzos, N., 2000, *A&A*, **359**, 191.
 Gustafsson, B., Bell, R. A., Eriksson, K., Nordlund, A. 1975, *A&A*, **42**, 407.
 Howlveger, H. and Muller, E. A., 1974, *Solar Phys.*, **39**, 19.
 Jacoby, G. H., Hunter, D. A., Christian, C.A., 1984, *ApJS*, **56**, 257.
 Kurucz, R.L. 1993, ATLAS9 Stellar Atmosphere Programs and 2km s⁻¹ grid CDRoM, Vol 13 (Cambridge: Smithsonian Astrophysical Observatory).
 Lebreton, Y., Perrin, M. N., Cayrel, R., Baglin, A., Fernandes, J., 1999, *A&A*, **350**, 587.
 Morgan, W.W., Keenan, P.C. and Kellman, E. 1943, An Atlas of Stellar Spectra with an Outline of Spectral Classification. Univ. of Chicago Press.
 Prabhu, T.P., Anupama, G. C., Surendiranath, R. 1998, *BASI*, **26**, 383.
 Sneden, C. 1973, Ph.D. Thesis Univ. of Texas at Austin.
 Schmidt-Kaler, Th. 1982, In Numerical data and Functional Relationships in Science and Technology, Editors K. Schaifers and H.H. Vogt (Springer-Verlag)

- Stobie, R. S., Kilkenney, D., O'Donoghue, A. et al. 1997, *MNRAS*, **287**, 848.
Thevenin, F., 1989, *ApJS*, **77**, 137.
Thevenin, F., 1990, *A&AS*, **82**, 179.